Chemical Science

EDGE ARTICLE

View Article Online
View Journal | View Issue

Cite this: *Chem. Sci.*, 2014, **5**, 2862

Practical synthesis of water-soluble organic nanoparticles with a single reactive group and a functional carrier scaffold†

Yugang Bai,[a] Hang Xing,[ab] Gretchen A. Vincil,[a] Jennifer Lee,[a] Essence J. Henderson,[a] Yi Lu,[ab] N. Gabriel Lemcoff[c] and Steven C. Zimmerman*[a]

Received 7th March 2014
Accepted 21st April 2014

DOI: 10.1039/c4sc00700j

www.rsc.org/chemicalscience

A new approach to prepare functional organic nanoparticles (ONPs) from linear polymers is described. The nanoparticles are obtained by ring-opening metathesis polymerisation (ROMP) of functionalised norbornene dicarboximides, side-chain amidation with tri-*O*-allyl-TRIS, and ring-closing metathesis (RCM). The synthesis is quite flexible and mild, allowing preparation of organic- and aqueous-soluble particles with narrow molecular weight (MW) distributions that are tunable, ranging from MW ≈ 10 to >100 kD with diameters between *ca.* 5 and 50 nm. The use of functional monomer(s) and/or chain-transfer agents (CTAs) leads to the fully controlled synthesis of nanoparticles containing single or multiple reactive functional groups. This non-toxic ONP scaffold can be readily used as a protective carrier for a broad range of groups using the appropriate monomers, such as a fluorescein-functionalised monomer that affords fluorescent ONPs with significantly enhanced photostability.

Introduction

The recent intense interest in organic nanoparticles (ONPs) originates in large part in their many real and potential applications in materials (*e.g.*, inks, cosmetics), catalysis, electronics, photonics, bioimaging and drug delivery. Typical ONPs have dimensions between 10 nm and 1 μm.[1] The traditional preparation of ONPs involves nanoprecipitation or emulsion polymerisation methods.[2] Considerable attention has also focused on "top-down" approaches to prepare smaller ONPs in the 5 to 50 nm range, which are more suitable for photonic and biological applications. These methods include the use of microfluidics, laser ablation, and other strategies to afford smaller and more uniform ONPs.[3] A potentially powerful alternative involves the intramolecular cross-linking of polymers, a strategy successfully applied to dendrimers,[4] and to star,[5] hyperbranched,[6] and linear[7] polymers.

As illustrated schematically in Fig. 1, the most useful synthetic approach would allow control over the ONP: (1) size, (2) hardness (*i.e.*, flexibility), (3) solubility, (4) external functionality, (5) internal functionality, and (6) density/porosity, as well as being (7) scalable and (8) producing ONPs of low toxicity and high biocompatibility for bio-applications and low environmental impact. Finally, having a single reactive functional group on the ONP surface is very useful for controlled nanoscale assembly[8] and two orthogonally reactive functional groups[9] would provide access to an even broader set of applications.

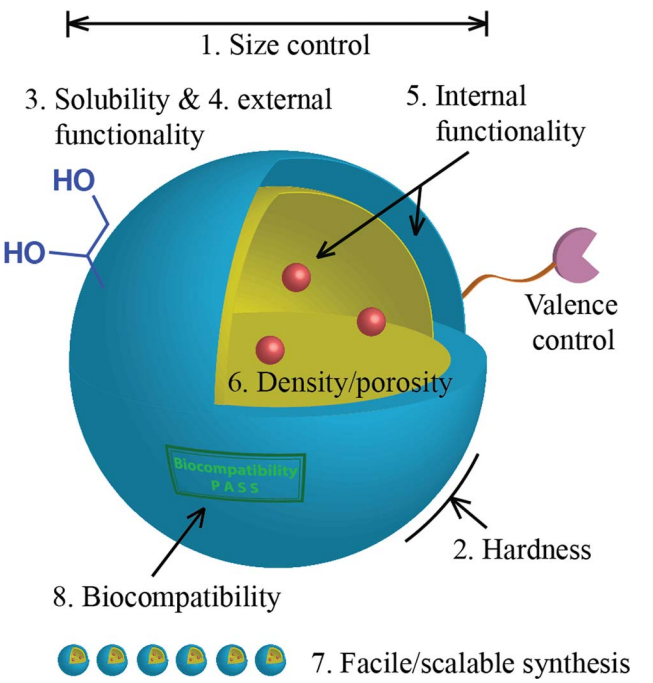

Fig. 1 Schematic illustration of idealized organic nanoparticles with desired features for applications.

[a]*Department of Chemistry, University of Illinois at Urbana-Champaign, Urbana, Illinois 61801, USA*

[b]*Beckman Institute, University of Illinois at Urbana-Champaign, Urbana, Illinois 61801, USA*

[c]*Department of Chemistry, Ben-Gurion University of the Negev, Beer-Sheva 84105, Israel*

† Electronic supplementary information (ESI) available: Experimental details, including synthesis and characterisation of monomers and polymers, are available in the ESI. See DOI: 10.1039/c4sc00700j

Obtaining ONPs with a limited number of reactive groups is a particular challenge because nanoparticles are invariably prepared with a large number of identical groups on their surface. It may be possible to borrow strategies developed for preparing monovalent metal nanoparticles, although these do have some limitations, particularly with regard to scalability. The successful strategies for generating monovalent metal NPs involve statistical surface functionalisation followed by fractionation or separation steps, or reaction of the NP with a reactive surface.[10] A very specialized approach for gold nanoparticles involves placing two reactive groups on polar opposite positions of the surface coated with a mixed monolayer.[11]

With regard to the list above, most of the reported approaches to ONPs offer control over just a few of these properties. Dendrimers are an exception, offering readily tunable sizes and the ability to place a wide range of functionality at the periphery and within the branching units. However, dendrimers require multi-step syntheses making scalablity an issue, and the elegant syntheses of mono- and bivalent dendrimers[12] require even longer syntheses. The strategy of cross-linking linear polymers[7] appears particularly attractive because it can produce ONPs with readily controlled molecular weight, cross-link density, polydispersity, and functionality. Indeed, the main limitation in these ONPs reported to date is a lack of water solubility and functionality for further manipulation.

Herein we describe a new synthetic approach to ONPs. The key to the strategy is the use of the ring-opening metathesis polymerisation (ROMP) of functionalised norbornene dicarboximides **1**, catalysed by pyridine-modified Grubbs catalyst **2** (commonly referred as Grubbs 3rd generation catalyst).[13] This catalyst is highly functional group tolerant allowing a range of functionality to be placed on the ONP scaffold. At the same time, precise control over chain length and polydispersity is provided, as well as straight-forward chain-end functionalisation using chain-transfer agents (CTAs). Importantly, ROMP is the only living polymerisation technique that generates unsaturated polymers whose high alkene content allows dihydroxylation, yielding non-ionic, hydrophilic back-bones with high aqueous solubility. The ROMP was paired with a ring-closing metathesis (RCM) reaction, allowing cross-linking under mild conditions, as well as producing an additional set of alkenes. Using these metathesis reactions in sequence followed by dihydroxylation has led to an ONP synthesis that possesses nearly all of the attributes illustrated in Fig. 1.

Experimental section

All monomers used in this study were synthesized from commercially available *cis*-5-norbornene-*endo*-2,3-dicarboxylic anhydride. General procedures for the synthesis of monomers and CTAs, as well as polymerisation and post-functionalisation procedures and cell studies can be found in the ESI.†

Results and discussion

Our initial approach examined a tandem ROMP-RCM process using monomer **1** with pendant alkene moieties. This single step approach to ONPs is appealing; however, despite investigating multiple monomers with different types of alkene groups, either the ROMP or RCM step proved to be problematic due to cross-reactivity. As outlined in Scheme 1, a sequential process, wherein the alkene groups for RCM are added in a second step, was developed to bypass the possibility of cross-reactivity. Thus, each ROMP was carried out with monomer **1a** carrying an activated ester and a comonomer, initially **1b**. The ROMP proceeded smoothly to give the corresponding poly(*endo*-norbornenes) **3** with low polydispersity indices (PDIs) and a range of molecular weights that could be readily controlled by setting the initiator to monomer ratio (Table 1 and ESI†). Treatment of **3** with tri-*O*-allyl-TRIS (**4**) afforded polymer **5** displaying a large number of allyl groups along its backbone. The ^{1}H NMR of **5** showed a complete absence of the succinimidyl group indicating that within the detection limit of NMR, the activated esters were fully converted to the amide. Nitrobenzene was used as a cosolvent in the amidation reaction to suppress radical mediated cross-linking of the allyl groups,[14] which was previously observed with allylated polyglycerol dendrimers.[6] The intramolecular crosslinking (RCM) of **5** was effected using **6** (Grubbs 1st generation catalyst),[15] whose lower reactivity avoided intermolecular metathesis during work-up.[4,5] Performing the RCM reaction under dilute conditions allowed formation of the ONPs with little or no dimeric material observed. Evidence for fully cross-linked ONPs was readily observed in the ^{1}H NMR.

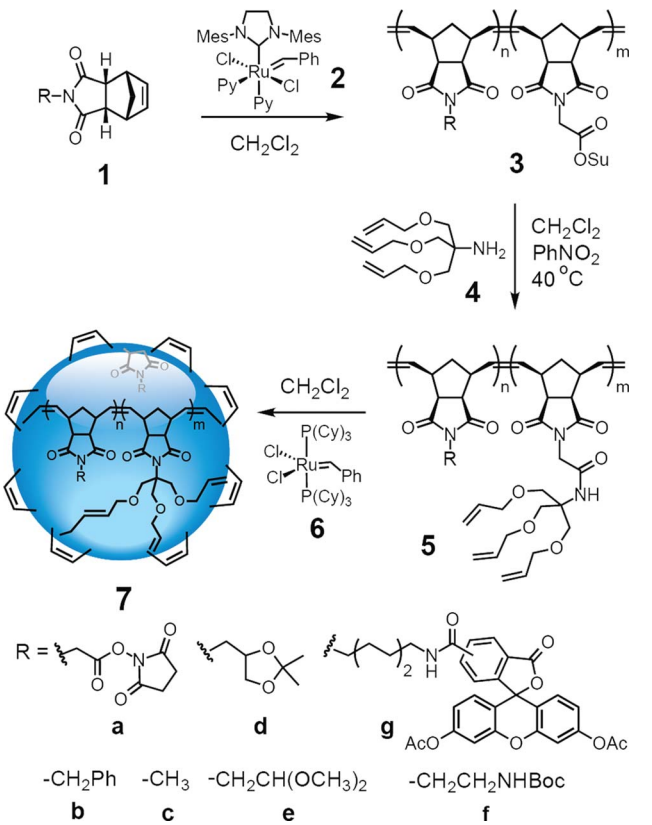

Scheme 1 Synthesis of organic nanoparticles (ONPs) using a sequential ROMP and RCM process. Py = pyridine, Mes = 2,4,6-trimethylphenyl, OSu = *N*-hydroxysuccinimidyl ester.

Table 1 Representative characterization data for polymers synthesized in this work

Entry	Comonomer	M/I ratio[a]	CTA (eq.)	Polymer 3 Mn[b] (kDa)	Polymer 3 PDI	Polymer 5 Mn (kDa)	Polymer 5 PDI	ONP 7 Mn (kDa)	ONP 7 PDI	Additive during RCM (equiv.)
1	**1b**	50/100/1	None	39.8	1.09	48.9	1.10	48.3	1.13	None
2	**1c**	75/150/1	None	49.0	1.03	59.5	1.09	57.5	1.20	None
3	**1c**	50/100/1	**9a** (5)	ND[c]	ND	43.2	1.12	42.7	1.28	None
4	**1c**	25/50/1	**9b** (5)	17.0	1.03	21.8	1.03	15.1	1.05	None
5	**1c**	50/100/1	**9b** (5)	37.6	1.04	45.9	1.06	NA[d]	1.07[e]	**10** (5)
6	**1c**	75/150/1	**9b** (5)	53.6	1.05	69.9	1.15	67.1	1.22	None
7	**1e**	50/100/1	None	42.0	1.08	49.1	1.09	47.3	1.13	None

[a] Molar ratio of **1a**/comonomer (**1*x***, ***x*** can be **b**–**g**)/**2**. [b] Absolute number-average molecular weight determined by a GPC with a multi-angle laser light scattering (MALLS) detector. [c] Not determined. [d] Interference of fluorescence in MALLS detection prevented absolute molecular weight determination, but polystyrene calibration gave similar "molecular weight shrinking" compared to other entries. [e] Polydispersity was calculated by Breeze 2 software from Waters Corporation based on RI data and traditional polystyrene calibration method.

Thus, the terminal alkene CH groups that appear between δ 5.0–5.5 ppm in **5** are replaced by a broad peak at 5.7 ppm in the spectrum of **7**, consistent with the formation of 1,2-disubstituted alkene groups (see Fig. 2a).

The GPC analysis was also consistent with extensive intramolecular cross-linking. Thus, whereas the conversion of **3** to **5** gave a small shift to a shorter retention time consistent with an increase in size, the RCM product **7** gave a single peak that eluted significantly later (Fig. 2b). The molecular weight of **7** determined by conventional calibration gave much smaller values than expected for loss of ethylene units from **5**, reflecting its collapsed, cross-linked structure. In contrast, multi-angle laser light scattering (MALLS) detection gave a more accurate assessment of the true molecular weight of the polymers; thus the M_n value for **7** was found typically only about 1–4% lower than the M_n obtained for **5** (Table 1).

ONP **7** was very soluble in several common organic solvents. In an effort to render these particles water-soluble, monomers **1c** and **1d** were synthesized and used in the copolymerisation with **1a**. These two new monomers formed polymer **5** and ONP **7** in the same manner as **1b** did, showing the versatility of the synthetic strategy. The large number of alkene groups in **7**, arising from both the ROMP and RCM steps, allowed use of dihydroxylation chemistry to prepare water-soluble ONP. Using the Upjohn conditions,[16] *i.e.*, *N*-methylmorpholine-*N*-oxide (NMO) and K_2OsO_4 in acetone–water at slightly elevated temperature (313 K), led to ONP that were fully soluble in water but not in organic solvents, even DMF (Fig. 3a). The ONP containing monomer **1d** were hydrolysed in aqueous hydrochloric acid to provide additional diol units. In each case the ^{1}H NMR spectrum in D_2O revealed complete disappearance of the alkene peaks, indicating complete oxidation of the double bonds (see ESI†). Finally, the overall synthetic approach outlined in Scheme 1 and Fig. 3a was shown to be sufficiently versatile to allow gram quantities of ONPs **8** to be prepared (see Fig. 3b).

To determine the shape of the ONPs prepared in this study and provide direct information about their sizes, transmission electron microscopy (TEM) was performed on three separate batches of ONPs **8** with different sizes. The polymers were prepared using monomer to initiator ratio for **1a** : **1d** : **2** = 100 : 200 : 1, 50 : 100 : 1, and 10 : 20 : 1, giving water-soluble ONPs whose post-dihydroxylation molecular weights were 102, 53, and 12 kDa, respectively. These values were calculated from the GPC-MALLS determined molecular weights of the corresponding parent polymers (see ESI†) and complete dihydroxylation. As seen in Fig. 4, the ONP are roughly spherical with diameters ranging from *ca.* 5–10 nm up to *ca.* 50 nm.

The copolymerisation approach described above with functional monomers such as **1e** and **1f** and subsequent cross-linking and dihydroxylation smoothly produces a wide range of

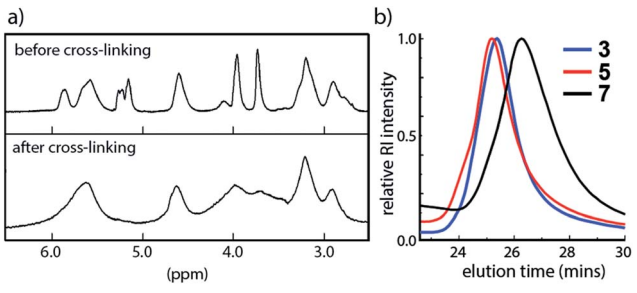

Fig. 2 (a) Partial ^{1}H NMR spectra of **4** (top) and **7** (bottom) showing loss of terminal alkene; (b) overlaid GPC curves of polymers **3**, **5**, and **7** (DMF, 0.1 M LiBr, eluent). Both (a) and (b) are from polymers prepared in entry 1, Table 1.

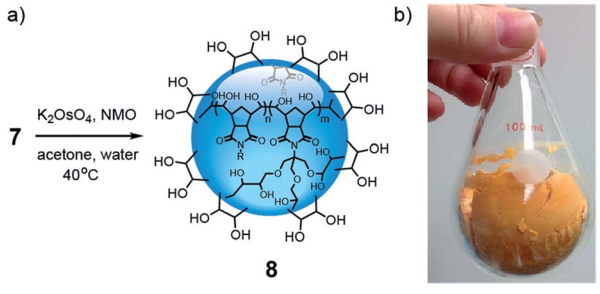

Fig. 3 (a) Dihydroxylation protocol to generate water-soluble ONPs; (b) example of gram-scale preparation of ONP **8**. Sample in the picture contains a M/I ratio of **1a** : **1d** : **1f** : **2** = 100 : 50 : 4 : 1. Note: *exo*-norbornene monomers used.

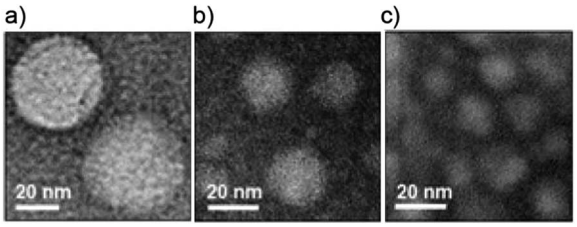

Fig. 4 Selected TEM images of water-soluble ONPs of different sizes. The polymer M_n values are (a) 102 kDa, (b) 53 kDa, and (c) 12 kDa. For a broader selection of images see ESI (Fig. S7†). These ONPs were end-functionalised with CTA **9b** (see next page).

ONPs with multiple hydroxyl groups on their surfaces and interiors. This same "bottom-up" approach appeared to offer a special opportunity to integrate in a single, uniquely reactive functional moiety into the nanoparticle. The general strategy used is shown in the preparation of ONPs **7** and **8**. Thus, the living nature of the ROMP process allows the use of a chain-transfer agent (CTA) to cap the end of the polymer chain directly,[13,17] producing a monovalent ONP (Scheme 2). Toward this end, three CTAs, **9a–c**, were prepared and added to the reaction mixture at the end of the ROMP. The mono-functionalisation was confirmed by ^{1}H NMR analysis prior to the RCM-mediated cross-linking.

To demonstrate the reactivity and accessibility of the functional group of the monovalent ONP, a 21.8 kDa ONP, **7** (entry 4, Table 1) prepared using CTA-2 (**9b**) was conjugated to a 10 kDa thiol-functionalised mPEG as outlined in Scheme 2. Thus, the NHBoc-containing polymer was treated by trifluoroacetic acid in dichloromethane and the resulting amine reacted with sulfo-succinimidyl-4-(*N*-maleimidomethyl)cyclohexane-1-carboxylate (sulfo-SMCC), followed by mPEG-SH addition in a DMF–water mixture. Unreacted ONPs were removed by filtration, and unreacted mPEG molecules were removed by successive washing and filtering through a 30 kDa cutoff Amicon membrane. The mPEG conjugation was immediately apparent given that the functionalised ONPs became soluble in water.

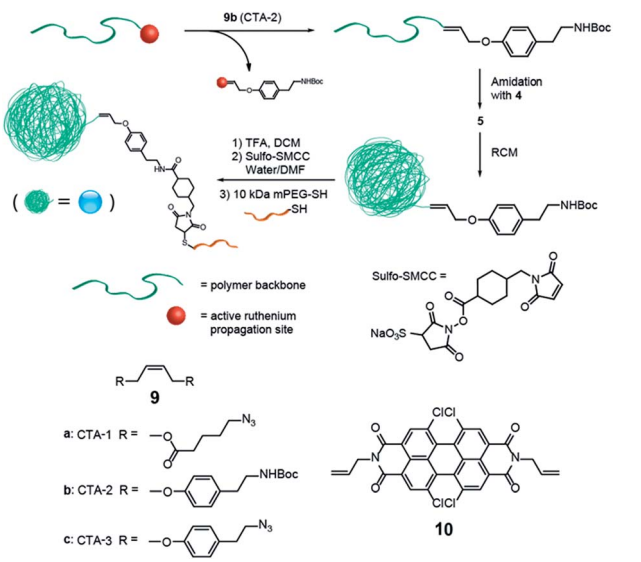

Scheme 2 Schematic illustration of the synthesis of monovalent ONPs using CTAs, and further functionalisation pathways using RCM or facile bioconjugation reactions.

Beyond effecting RCM reactions, Grubbs catalyst **6** is able to mediate olefin cross-metathesis. Because a common catalyst is used for these two processes, it suggested the possibility of integrating in new functionality during the cross-linking process (*i.e.*, RCM of **5** to **7**). To test this possibility, perylenediimide **10** was prepared from allylamine and 1,6,7,12-tetrachloroperylene-3,4,9,10-tetracarboxylic acid dianhydride. Perylenediimide **10** was added to the reaction mixture at the beginning of the RCM process, otherwise the overall ONP preparation was identical to that previously described. The resultant perylenedimide-containing polymer **7** (entry 5, Table 1) was fluorescent and exhibited a low PDI. The GPC trace from the UV detector showed a peak with an identical shape and elution time to that from the RI detector. Fluorescent polymer **7** underwent dihydroxylation using the conditions in Fig. 3a, yielding water-soluble, fluorescent ONP **8** after purification *via* dialysis (see ESI†).

The preparation of fluorescent nanoparticles containing the perylenediimide unit is one application of the chemistry described herein. There was particular interest in the ability of the ONP to reduce the photobleaching that plagues nearly all organic fluorophores. Indeed, a continuing challenge is to prepare bright and stable fluorescent probes,[18] especially useful being those that are monovalent for specific biolabeling.[19]

To test the possibility that that the polymeric framework of **8** might increase fluorophore stability, ONP **8** containing fluorescein units were prepared using monomer **1g**. Fluorescein was chosen as a widely used fluorophore that is especially prone to photobleaching.[20] A fully water-soluble 28 kD ONP **8** was prepared using CTA-2 (**9b**) as an end-cap and with an average of four fluorescein units. As seen in Fig. 5a, the ONP is visibly brighter than fluorescein at a similar concentration. More importantly, its performance over time is significantly improved indicating the protective effect of the ONP (Fig. 5a and b). Furthermore, because the loading of the fluorescein groups within the ONP is readily controlled simply by tuning the equivalents of **1g** used in the ROMP, brighter ONPs could be prepared as shown in Fig. 5c. Indeed, as the equivalents of the fluorescein monomer were increased during polymerization, a linear increase in ONP fluorescence intensity was observed when the dye loading was not too high. This experiment further illustrates how the loading of a moiety of interest may be easily and accurately controlled simply by tuning the M/I ratio. The origin of the protection effects is under investigation as are efforts to optimise the performance of these types of fluorescent ONP, including understanding the relationship between the different tunable aspects of the ONP: its size, number of fluorophores, degree of cross-linking.

Having demonstrated the exceptional photostability of the fluorescein ONPs, we then investigated their ability to enter live HeLa cells (human cervical canceras) as a nanoscale delivery and imaging system for potential intracellular theranostic applications (Fig. 6a). Fluorescein ONPs (**1a : 1d : 1g**

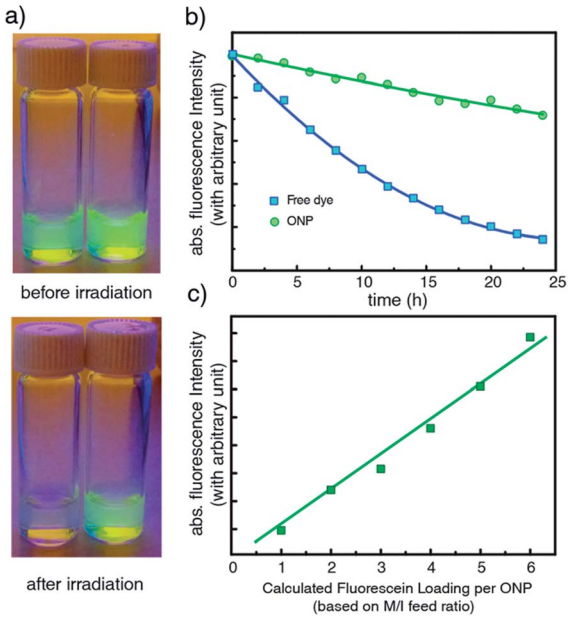

Fig. 5 (a) Photobleaching study using 470 nm LED with fluorescein (1 μM, left vial) and ONP **8** (1 μM, right vial) before and after irradiation in pH 7.4 phosphate buffer; (b) relative fluorescence of fluorescein and ONP **8** over time during the photobleaching experiment; (c) accurate tuning of ONP fluorescence intensity by adjusting the equivalents of fluorescein monomer **1g** during ROMP.

ratio = 10 : 20 : 4, *ca.* 12 kDa) were synthesized and incubated with HeLa cells for 6 h before further characterizations. As shown in Fig. 6b–f, HeLa cells treated with ONPs exhibited bright green fluorescence inside cells under confocal microscope, indicating the great internalization of ONPs. To study the intracellular distribution of ONPs, LysoTracker red was used to stain the lysosomes of HeLa cells. The good co-localization of fluorescence from ONPs and LysoTracker demonstrate that the ONPs are mainly transported to the lysosomes of HeLa cells, suggesting a receptor-mediated endocytosis process.

To further ensure that the observations through confocal microscope apply to whole cell population, quantitative fluorescence analysis for whole cell population was examined using flow cytometry for HeLa cell samples with or without ONPs treatment. The result shows that HeLa cells treated with green fluorescence ONPs had a more than 100-fold higher level of fluorescence than untreated cells (Fig. 6g), which is consistent with the observations under confocal microscope, confirming the uptake of ONPs. The demonstrated excellent photostability and cellular uptake features of these ONPs suggest their use in future applications such as long-term bioimaging and continuous tracking of living cells.

One potential concern given the heavy metal-containing reagents used in the synthesis of ONP **8** is the presence of residual osmium and ruthenium. Indeed, the ICP analyses showed significant levels of both. Preliminary studies showed that treating solutions of **8** with a polyvinylpyridine-based resin such as Smopex-105 reduced the metal ion contamination to parts per million levels. Even before treatment with the coordinating resin, ONP **8** ranging from *ca.* 10–100 kDa exhibited

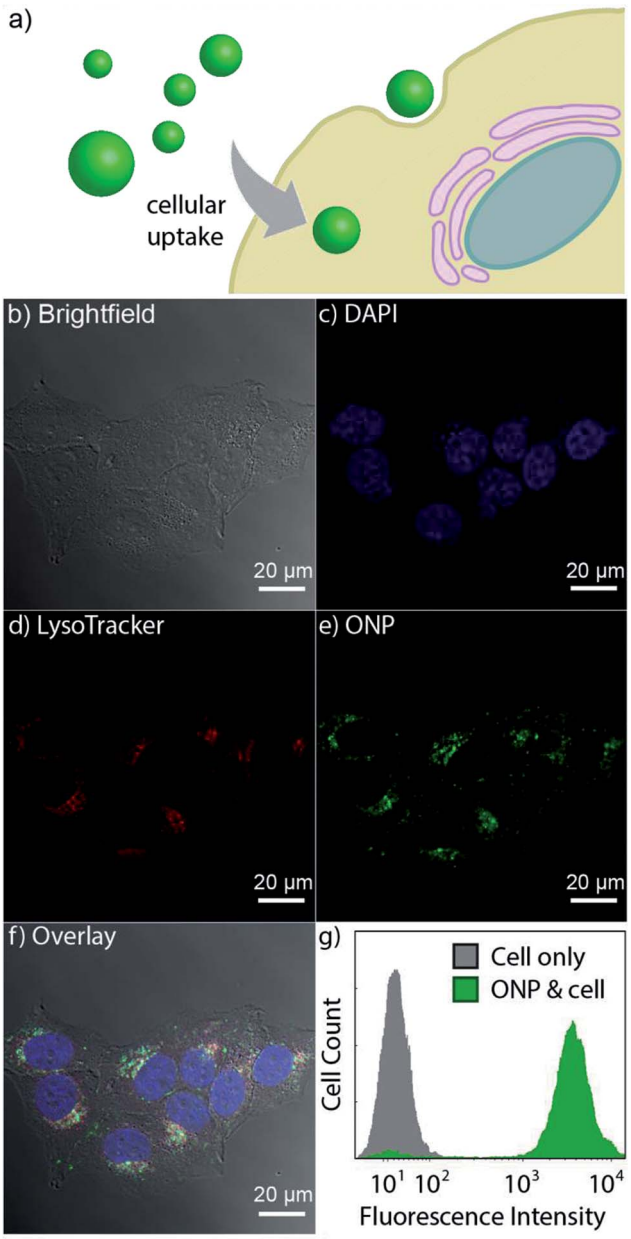

Fig. 6 (a) Schematic view of the 12 kDa green fluorescent ONPs entering HeLa cells. (b–f) Confocal microscopy images of HeLa cells treated with 12 kDa green fluorescent ONPs: (b) brightfield image of cells; (c) blue channel image showing nucleus staining with DAPI; (d) red channel image showing LysoTracker red staining; (e) fluorescein fluorescence from ONPs; (f) overlay of nucleus, LysoTracker red and ONP fluorescence; (g) the cell-associated fluorescence intensities of HeLa cells (grey) and fluorescent ONPs (green) treated HeLa cells using flow cytometry.

MTT HeLa cell viabilities of ≥80% at a concentration of 10 μM (approximately 1 mg mL^{-1}) (See ESI, Fig. S10†).

Conclusion

We have described a new route to ONPs using sequential living ROMP and RCM reactions. By adjusting parameters of the living ROMP, the molecular weight and size of the ONP could be

precisely controlled with excellent PDI values in each case. The overall synthetic strategy is capable of producing gram quantities of product quite flexibly and under mild conditions, allowing a range of functional groups to be integrated controllably and covalently into the ONP during the ROMP, RCM, or post-functionalisation step. Indeed, one application demonstrated was the ability of the ONPs to carry multiple fluorescent probes and significantly increase their photostability.

A major advantage of this approach is the ability to produce mono- or poly-functional ONPs that are either organic or water-soluble. The capability of embeding a wide range of groups into the poly(norbornene) backbone suggest that numerous additional applications including light harvesting, multiplexed bioimaging and drug delivery might be possible using the single-chain particle approach described herein. These and other applications are under active investigation and will be reported in due course.

Conflict of interest

The authors declare no competing financial interest.

Acknowledgements

Funding from the Binational Science Foundation (2010047), the National Institutes of Health (GM087448), and the National Science Foundation (CHE-1307404) is gratefully acknowledged.

Notes and references

1 *Single Organic Nanoparticles*, ed. H. Masuhara, H. Nakanishi and K. Sasaki, Springer, Berlin, 2003.

2 J. Allouche, Synthesis of Organic and Bioorganic Nanoparticles: An Overview of the Preparation Methods. in *Nanomaterials: A Danger or a Promise?*, ed. R. Brayner, F. Fiévet and T. Coradin, Springer, Berlin, 2013, pp. 27–74.

3 T. Asahi, T. Sugiyama and H. Masuhara, *Acc. Chem. Res.*, 2008, **41**, 1790; A. Jahn, J. E. Reiner, W. N. Vreeland, D. L. DeVoe, L. E. Locascio and M. Gaitan, *J. Nanopart. Res.*, 2008, **10**, 925; P. Guo, C. R. Martin, Y. Zhao, J. Ge and R. N. Zare, *Nano Lett.*, 2010, **10**, 2202.

4 M. S. Wendland and S. C. Zimmerman, *J. Am. Chem. Soc.*, 1999, **121**, 1389; L. G. Schultz, Y. Zhao and S. C. Zimmerman, *Angew. Chem., Int. Ed.*, 2001, **40**, 1962; N. G. Lemcoff, T. Spurlin, A. A. Gewirth, S. C. Zimmerman, J. B. Beil, S. L. Elmer and H. G. Vandeveer, *J. Am. Chem. Soc.*, 2004, **126**, 11420; J. B. Beil, N. G. Lemcoff and S. C. Zimmerman, *J. Am. Chem. Soc.*, 2004, **126**, 13576.

5 J. B. Beil and S. C. Zimmerman, *Macromolecules*, 2004, **37**, 778.

6 S. C. Zimmerman, J. R. Quinn, E. Burakowska and R. Haag, *Angew. Chem., Int. Ed.*, 2007, **46**, 8164; E. Burakowska, J. R. Quinn, S. C. Zimmerman and R. Haag, *J. Am. Chem. Soc.*, 2009, **131**, 10574.

7 Non-covalent examples: E. J. Foster, E. B. Berda and E. W. Meijer, *J. Am. Chem. Soc.*, 2009, **131**, 6964; T. Mes, R. van der Weegen, A. R. A. Palmans and E. W. Meijer, *Angew. Chem., Int. Ed.*, 2011, **50**, 5085, covalent examples: E. Harth, B. V. Horn, V. Y. Lee, D. S. Germack, C. P. Gonzales, R. D. Miller and C. J. Hawker, *J. Am. Chem. Soc.*, 2002, **124**, 8653; A. E. Cherian, F. C. Sun, S. S. Sheiko and G. W. Coates, *J. Am. Chem. Soc.*, 2007, **129**, 11350, For recent review with lead references see: M. Ouchi, N. Badi, J.-F. Lutz and M. Sawamoto, *Nat. Chem.*, 2011, **3**, 917.

8 P. S. Weiss and C. Mirkin, *ACS Nano*, 2009, **3**, 1310.

9 C.-H. Wong and S. C. Zimmerman, *Chem. Commun.*, 2013, **49**, 1679.

10 Selected reports on the preparation of monovalent nanoparticles: D. Zanchet, C. M. Micheel, W. J. Parak, D. Gerion and A. P. Alivisatos, *Nano Lett.*, 2001, **1**, 32; J. G. Worden, A. W. Shaffer and Q. Huo, *Chem. Commun.*, 2004, 518; Q. Dai, J. G. Worden, J. Trullinger and Q. Huo, *J. Am. Chem. Soc.*, 2005, **127**, 8008.

11 G. A. DeVries, M. Brunnbauer, Y. Hu, A. M. Jackson, B. Long, B. T. Neltner, O. Uzun, B. H. Wunsch and F. Stellacci, *Science*, 2007, **315**, 358; Y. Ohya, N. Miyoshi, M. Hashizume, T. Tamaki, T. Uehara, S. Shingubara and A. Kuzuya, *Small*, 2012, **8**, 2335.

12 For some existing cases of monovalent or bivalent dendrimers, see: R. Stangenberg, I. Saeed, S. L. Kuan, M. Baumgarten, T. Weil, M. Klapper and K. Müllen, *Macromol. Rapid Commun.*, 2014, **35**, 152; C. Ornelas and M. Weck, *Chem. Commun.*, 2009, 5710; Z. Bo, A. Schäfer, P. Franke and A. D. Schlüter, *Org. Lett.*, 2000, **2**, 1645; W. Zhang, D. T. Nowlan III, L. M. Thomson, W. M. Lackowski and E. E. Simanek, *J. Am. Chem. Soc.*, 2001, **123**, 8914; R. N. Ganesh, J. Shraberg, P. G. Sheridan and S. Thayumanavan, *Tetrahedron Lett.*, 2002, **43**, 7217; G. Mihov, I. Scheppelmann and K. Müllen, *J. Org. Chem.*, 2004, **69**, 8029; K. Yoon, P. Goyal and M. Weck, *Org. Lett.*, 2007, **9**, 2051, and ref. 18.

13 T.-L. Choi and R. H. Grubbs, *Angew. Chem., Int. Ed.*, 2003, **42**, 1743; S. Hilf and A. F. M. Kilbinger, *Nat. Chem.*, 2009, **1**, 537.

14 H. Lu, Y. Bai, J. Wang, N. P. Gabrielson, F. Wang, Y. Lin and J. Cheng, *Macromolecules*, 2011, **44**, 6237.

15 R. H. Grubbs, S. J. Miller and G. C. Fu, *Acc. Chem. Res.*, 1995, **28**, 446; G. W. Coates and R. H. Grubbs, *J. Am. Chem. Soc.*, 1996, **118**, 229.

16 V. VanRheenen, R. C. Kelly and D. Y. Cha, *Tetrahedron Lett.*, 1976, **17**, 1973, For related systems, see: S. K. Yang and S. C. Zimmerman, *Adv. Funct. Mater.*, 2012, **22**, 3023 and ref. 6.

17 S. Hilf, R. H. Grubbs and A. F. M. Kilbinger, *J. Am. Chem. Soc.*, 2008, **130**, 11040; J. B. Matson, S. C. Virgil and R. H. Grubbs, *J. Am. Chem. Soc.*, 2009, **131**, 3355; Y. Bai, H. Lu, E. Ponnusamy and J. Cheng, *Chem. Commun.*, 2011, **47**, 10830.

18 Selected reviews: B. N. G. Giepmans, S. R. Adams, M. H. Ellisman and R. Y. Tsien, *Science*, 2006, **312**, 217; U. Resch-Genger, M. Grabolle, S. Cavaliere-Jaricot, R. Nitschke and T. Nann, *Nat. Methods*, 2008, **5**, 763; L. D. Lavis and R. T. Raines, *ACS Chem. Biol.*, 2008, **3**, 142; H. Kobayashi, M. Ogawa, R. Alford, P. L. Choyke and

Y. Urano, *Chem. Rev.*, 2010, **110**, 2620; T. Ha and P. Tinnefeld, *Annu. Rev. Phys. Chem.*, 2012, **63**, 595.
19 S. K. Yang, X. Shi, S. Park, S. Doganay, T. Ha and S. C. Zimmerman, *J. Am. Chem. Soc.*, 2011, **133**, 9964; S. K. Yang, X. Shi, S. Park, T. Ha and S. C. Zimmerman, *Nat. Chem.*, 2013, **5**, 692.
20 H. Giloh and J. W. Sedat, *Science*, 1982, **217**, 1252.